17th World Conference on Earthquake Engineering, 17WCEE
Sendai, Japan - September 13th to 18th 2020

CHARACTERISTICS OF INPUT MOTION FOR CASTLE

S. Fujii [1], T. Fujimori[2]

[1] *Chief, Technical Research Institute, OBAYAHI CORPORATION, fujii.satoru@obayashi.co.jp*
[2] *Senior Engineer, Technical Research Institute, OBAYAHI CORPORATION, fujimori.takeshi@obayashi.co.jp*
…

Abstract

Main purpose of this study is to analyze the influence of the masonry wall embankment on the input motion characteristics of the castle. It was analyzed by analysis using the finite element method (FEM) and microtremor measurement of the embankment imitating the masonry wall. It was mentioned as background that since the enactment of the Tourism Nation Promotion Basic Law in 2006, tourism has been positioned as one of the pillars of Japan's important measures, and there are many plans to rebuild the castle tower in cities which has historic castle sites. Amid these circumstances, it is important to evaluate appropriately the influence of the masonry wall embankment in the seismic response and secure the seismic performance of castles.

The main results about the characteristics of input motion for castle were follows;

(1) It is need to pay attention to underestimation due to modeling the masonry wall embankment as horizontally flat strata when the input motion of the castle was evaluated with a 1D ground model under the foundation,

(2) Regarding the seismic response of the ground, most of the castles in Japan might require attention to the above (1) when we considered the separation distance from the top of slope where the influence of embankment disappeared.

(3) The protrusion at the top of the masonry wall embankment had little effect on the earthquake response of the castle, because it had a small weight ratio to the whole embankment.

(4) There was no significant difference when we eliminated the stone weight on the surface of the masonry wall and evaluated the seismic response as a homogeneous embankment.

(5) When comparing microtremors and strong motions, the tendency of amplification at the embankment was similar. There was a difference in the tendency of amplification at the top of slope of the embankment. Hereafter, it is needs more detailed analysis since the tendency is likely to change depending on the shape of the embankment.

Keywords: Input Motion; Amplification Characteristics; FEM Analysis; Microtremor Measurement; Embankment

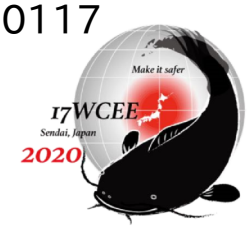

1. Introduction

Since the enactment of the Tourism Nation Promotion Basic Law in 2006, tourism has been positioned as one of the pillars of Japan's important measures, and many plans have been made to rebuild the castle towers in a city with a castle historic site. Amid these circumstances, it is important to evaluate appropriately the influence of masonry wall embankment in the seismic response and secure the seismic performance of castles.

In this study, we analyzed the effect of the masonry wall embankment on the characteristics of input motion for a castle by finite element method (FEM) analysis and microtremor measurement.

2. Analysis specifications

2.1 Analysis model

Most of the castles to be rebuilt and restored are classified into Hirajiro or Hirayamajiro in the center of the cities. So, the basic analysis model had a masonry wall embankment on the horizontally flat ground shown in Case-1 in Fig. 2.1. Analysis model was assumed to be a pile foundation because it was built on the embankment. In the simplest case of setting the input motion as in Case-1, it was likely to be a one-dimensional ground model under the foundation. Therefore, Case-4 was set as a 1D ground model corresponding to that simplest condition. Case-2 was a model in which masonry walls were eliminated for simplification and had only embankment. Case-3 was a slightly simpler model that was considered the protruding embankment (J1 part in the Fig. 2.1) that was put on the J2 part and beside the foundation in Case-4 that was the simplest case.

The foundation was a massless rigid foundation in each model. The depth width in the out-of-plane direction of the ground was set to 10.54*m*, which was the same as the foundation's depth. Table 2.1 and Table 2.2 showed the ground and the pile specifications. The piles were assumed to be cast-in-place piles (8 piles in total). Pile's nonlinear characteristics were taken as the modified Takeda model. Table 2.3 showed the non-linear characteristics of piles. In the analysis model, two piles in the depth direction were combined into one.

Rayleigh damping was set for each of the ground, piles, and a massless rigid foundation. The damping ratio was set to 2*%* for the primary and secondary natural frequencies (primary: 1.97 *Hz*, secondary: 2.74 *Hz*) obtained from the eigenvalue analysis.

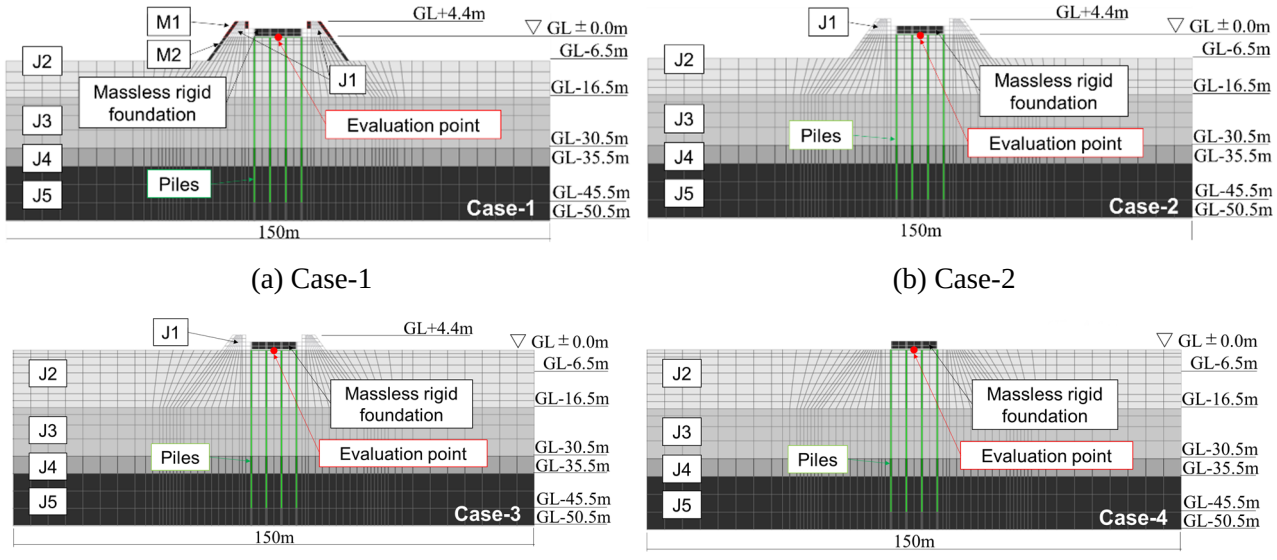

(a) Case-1 (b) Case-2

(c) Case-3 (d) Case-4

Fig. 2.1 – Analysis models and cases

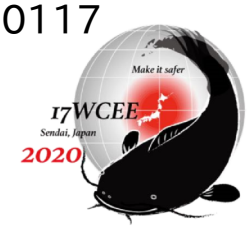

Table 2.1 – The ground specifications

No.	Geology	Velocity of S-wave V_S (*m/s*)	Velocity of P-wave V_P (*m/s*)	Unit weight ρ (kN/m^3)	Damping constant H	Dynamic response characteristics		Unit weight of the masonry wall	
						Reference strain $\gamma_{0.5}$	Maximum damping constant h_{max}	No.	(kN/m^3)
J1	Loam	160	330	17.1	0.02	0.0018	0.17	M1	26.5
J2	Mud lava	180	380	16.1	0.02	0.0018	0.17	M2	26.5
J3	Mud lava mixed with gravel pumice	380	850	15.0	0.02	0.0018	0.17	—	—
J4	Highly weathered tuff breccia	340	740	16.7	0.02	0.0018	0.17	—	—
J5	Weathered tuff breccia	410	929	18.1	0.02	—	—	—	—

Table 2.2 – The pile specifications

Diameter (*m*)	Cross-sectional areas (m^2)	Modulus of elasticity (kN/m^2)	Unit weight (kN/m^3)	Poisson's ratio ν
1.8	2.545	2.24E+07	24	0.2

Table 2.3 – The non-linear characteristics of piles

Crack strength	Yield strength		Ultimate strength	
Moment ($kN \cdot m$)	Moment ($kN \cdot m$)	Slope reduction rate	Moment ($kN \cdot m$)	Slope reduction rate
2.56E+03	4.03E+03	9.05E-02	4.19E+03	1.50E-02

2.2 The input seismic waves

The input seismic waves were three waves (Hachinohe NS phase, Random number phase, and JMA Kobe NS phase) that were adapted to the acceleration response spectrum of seismic ground motions that occur extremely rarely on engineering bedrock. That spectrum was specified in the Ministry of Construction's Notification No. 1461. Fig. 2.2 showed the time history of the input seismic waves.

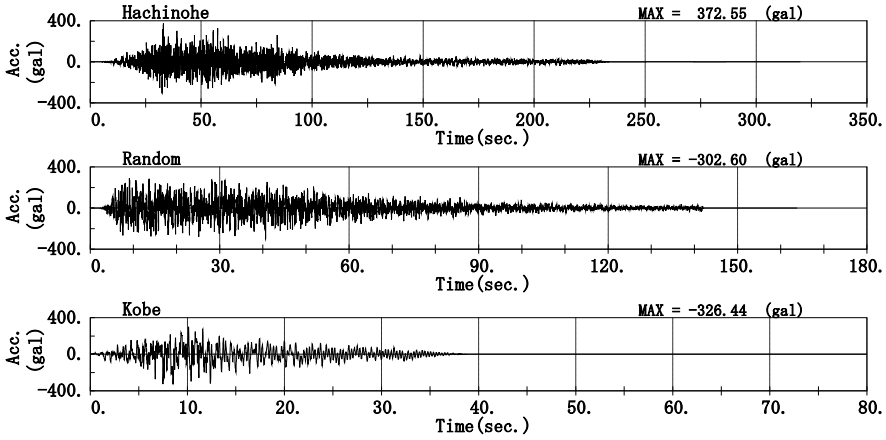

Fig. 2.2 – The input seismic waves

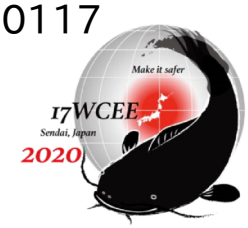

3. Evaluation of effects of masonry wall embankment

The results of FEM analysis were shown in Table 3.1 and Fig. 3.1. Table 3.1 was a comparison of the maximum response acceleration at the ground which was facing the bottom of the foundation (GL ± 0 m, Evaluation points in Fig. 2.1). The figures in parentheses indicate the magnification of Case-4. The maximum accelerations at the evaluation point were 621 to 683 *gal* in Case-1 and 2 and were 420 to 496 *gal* in Case-3 and 4. Case-1 and 2 showed 1.6 times larger than Case-3 and 4 in which the embankments were made into horizontally flat strata.

Fig. 3.1 showed a comparison of the acceleration response spectrum at the evaluation point. The difference between Case-1 which had masonry wall and Case-2 which had no masonry wall was small. The difference between Case-3 in which the protruding embankment was considered and Case-4 which had no embankment was also small. On the other hand, the period between 0.01 and 1 second, Case-1 and 2 showed larger spectra compared with Case-3 and 4. This difference had great influence on the castles on the masonry wall embankment because these castles were low-rise buildings and their natural period were less than 1 second. A method for correcting the cliff effect had been proposed in relation to the stratification of the embankment [1]. According to this method, the horizontal separation distance from the top of slope where the influence of embankment disappears was more than 10 times the embankment height.

Table 3.1 – Maximum acceleration (*gal*)

	Hachinohe	Random	Kobe
Case-1	621 [1.44]	683 [1.63]	667 [1.39]
Case-2	626 [1.46]	681 [1.62]	666 [1.39]
Case-3	455 [1.06]	450 [1.09]	496 [1.03]
Case-4	430 [1.00]	420 [1.00]	480 [1.00]

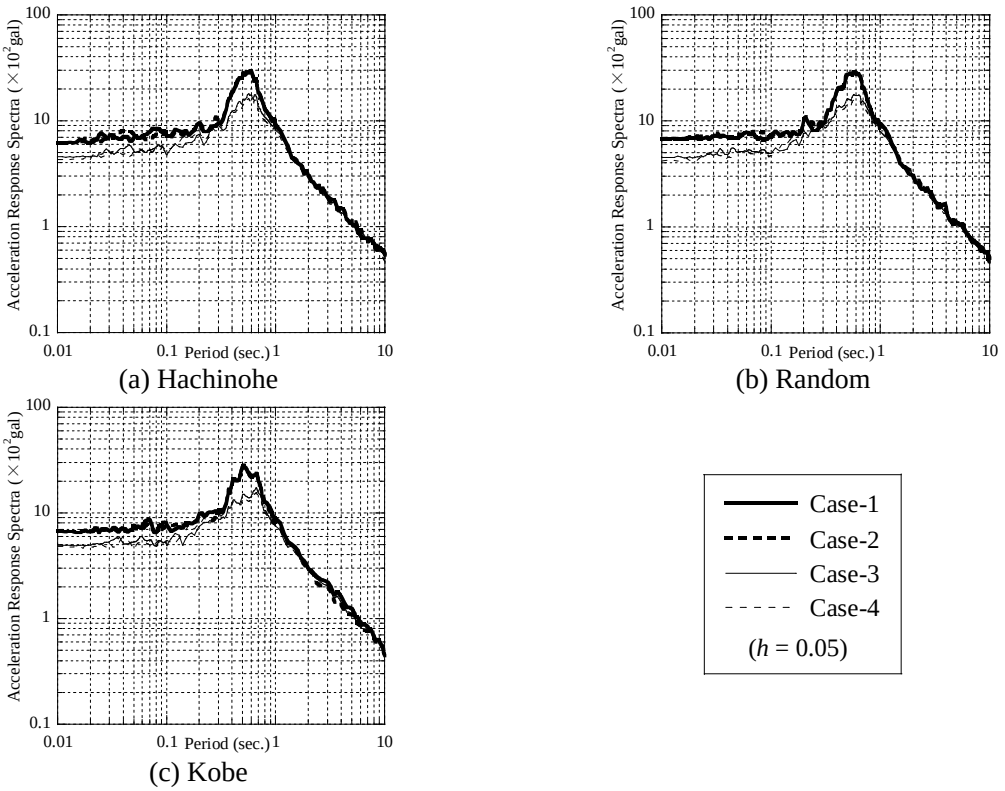

(a) Hachinohe (b) Random

(c) Kobe

Fig. 3.1 – Acceleration response spectra

4. Amplification characteristics of embankment based on microtremor measurement

In order to examine the application of the prediction by the microtremor measurement, it was analyzed that the results of actual microtremor measurement of the embankment.

4.1 The input seismic waves

Fig. 4.1 showed a side view and a plan view of the embankment and the arrangement of measurement point. The height of the embankment was approximately 1.6*m*, and the top of the embankment was approximately 6.5*m* x 3*m* with flat surface. The ground around the embankment was the Kanto loam layer it was deposited about 6*m* above the clayey gravel ground. The embankment was built on this ground using the loam.

Table 4.1 showed the specifications of the ground around the embankment. There are four measurement points, three on the top of embankment (P1 ~ 3) and one on the ground from 1.4m toe of slope of the embankment (G1).

The accelerations were measured simultaneously for 30 minutes using 100*Hz* sampling in three directions (east-west (EW), north-south (NS), and vertical (UD)) at all measurement points. The acceleration records were cut out 20 waveforms (40.96 seconds each) that had small traffic and walking vibrations.

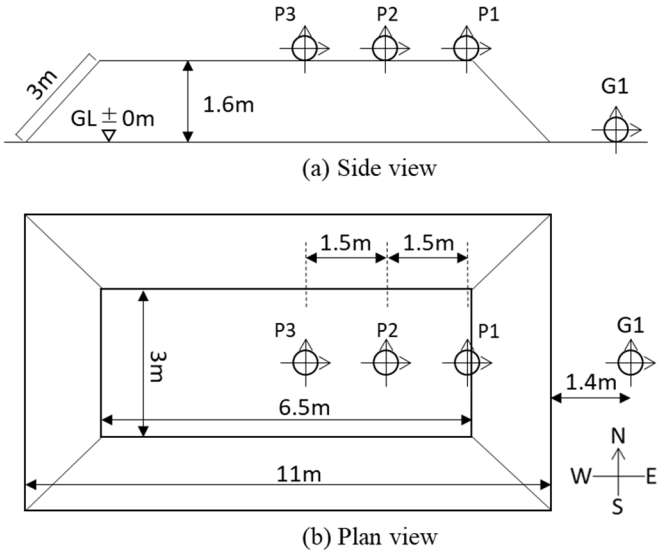

Fig. 4.1 – Overview of embankment and measurement points' arrangement

Table 4.1 – The ground specifications around the embankment

Top depth	Thickness (m)	Velocity of S-wave Vs (m/s)	Velocity of P-wave Vp (m/s)	Unit weight ρ (kN/m^3)	Poisson's ratio ν	Shear modulus G (kN/m^2)
GL±0.0m	2	150	360	14.3	0.396	3.281E+04
GL-2.0m	2	130	330	12.3	0.408	2.120E+04
GL-4.0m	2	160	420	12.3	0.415	3.211E+04

4.2 Results

Fourier spectrum was calculated by taking an arithmetic mean at each measurement point after Fourier-transforming the acceleration of 20 waves.

Figure 4.2 showed the Fourier spectra in the EW, NS and UD directions. From the results in the EW and NS direction, the peaks could be confirmed at approximately 5.4*Hz* that was the primary natural frequency in the horizontal direction of the surrounding ground. In the embankment part, another peak also could be confirmed at about 14 *Hz*, and this frequency was considered as the natural frequency of the embankment. On the other hand, in the UD direction, peaks could not be confirmed clearly like the horizontal direction.

Fig. 4.3 showed the H/V spectra in the EW direction. It could be confirmed that the ratio increased near the natural frequency of the embankment. In particular, the peak of amplification was remarkable at the top of slope (P1).

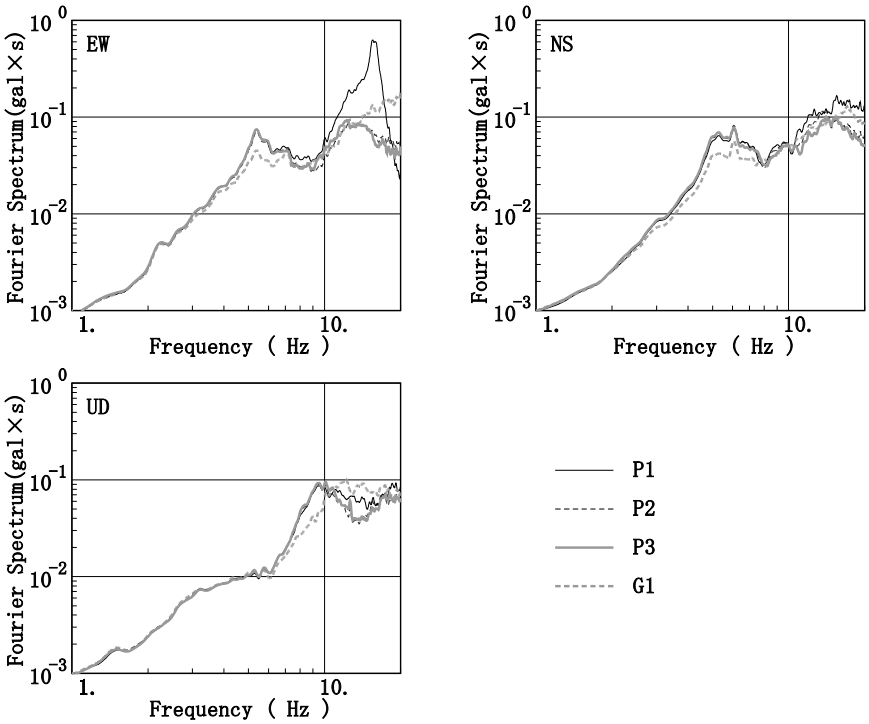

Fig. 4.2 –Fourier spectra (Arithmetic mean of 20 waves)

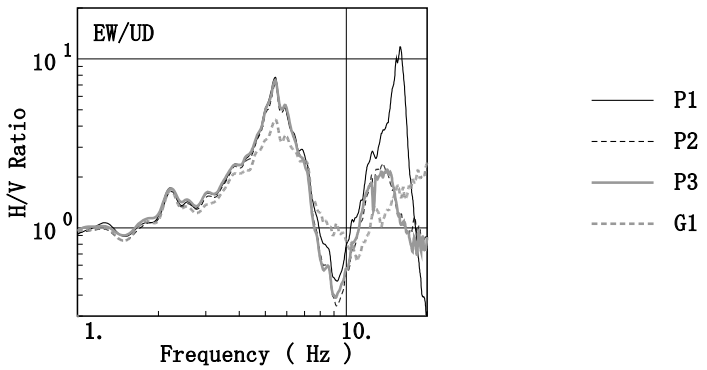

Fig. 4.3 – H/V spectra of EW direction (Arithmetic mean of 20 waves)

5. Analytical evaluation of amplification characteristics of embankment

In this chapter, the difference between microtremor and strong ground motion related to embankment behavior was analyzed by analytical evaluation based on the actual measurement analysis in the previous chapter.

5.1 Behavior of embankment in micro vibration

We analyzed the amplification characteristics of the embankment in detail by simulation analysis of microtremor measurement with time history. The embankment was modeled at the EW cross section with two-dimensional finite elements model (2D-FEM).

5.1.1 Analysis model

Fig. 5.1 showed the FEM model used for simulation analysis. The embankment was modeled to the actual size. The width of the ground was 36.5m. It was connected to the free field through a viscous boundary on the side. The bottom of the ground was also a viscous boundary. The response was evaluated at the 4 positions indicated by the crosses mark in the figure (Pa1~4 and Ga1). The specifications of the ground around the embankment were shown in Table 4.1. The specifications of the embankment were the same as the upper loam layer. The exciting point of the microtremor was shown in Fig. 5.1. It was assumed to be a road about 10 m away from toe of slope of the embankment.

The excitation force at the exciting point was calculated back by applying one wave measured at G1 in Fig. 4.1 to the surface ground model of the 3D thin layered element method analysis. The excitation force was performed in the horizontal direction. Fig. 5.2 showed the time history of the exciting force.

Rayleigh damping was set 2% for the primary and secondary natural frequency (primary:5.35 *Hz*, secondary: 15.09 *Hz*).

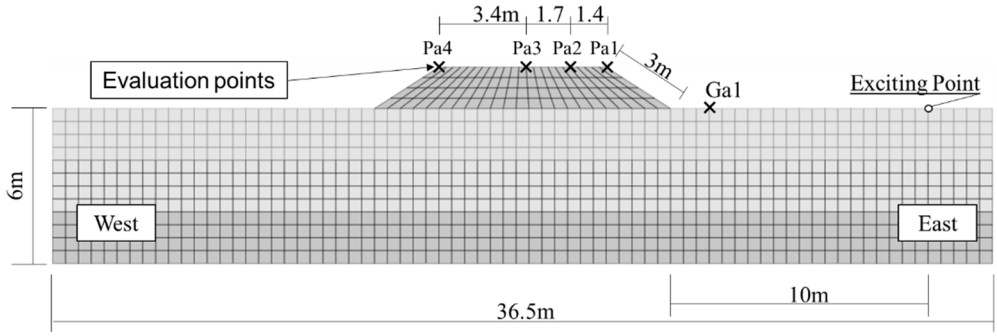

Fig. 5.1 – Analysis model

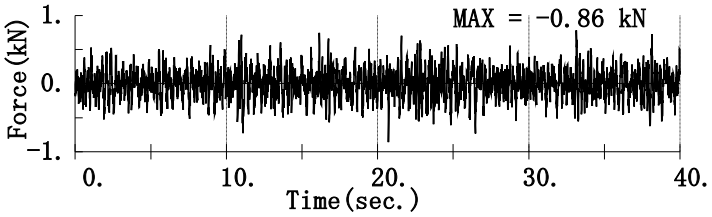

Fig. 5.2 – Exciting force wave

5.1.2 Analysis result

Fig. 5.3 compares the results of the measurement and analysis. Over 10Hz, including the natural frequency of the embankment, the results of observation and analysis were generally consistent. At frequencies lower than 10Hz, including the natural frequency of the surrounding ground, the consistency is slightly lower due to the point excitation of the ground surface.

Next, the detailed vibration characteristics of the embankment were confirmed from the distribution of maximum horizontally accelerations. The result was shown in Fig. 5.4. It could be confirmed that the embankment tended to increase the acceleration particularly at the top of slope.

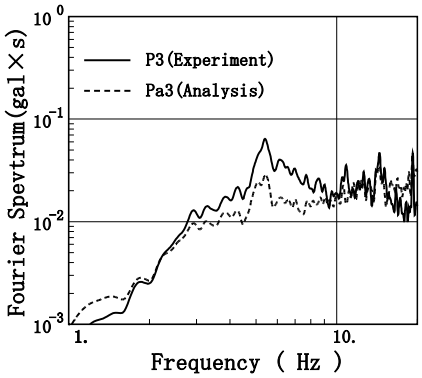

Fig. 5.3 – Comparison between analysis and measurement

(EW-Fourier spectra, Examination using one measured wave)

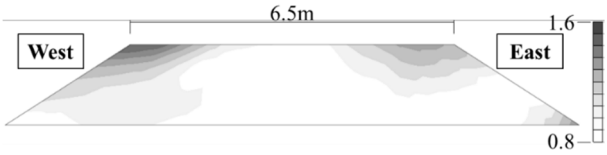

Fig. 5.4 – The distribution of maximum horizontally accelerations of the embankment (*gal*)

5.2 Behavior of embankment in large earthquake

Time history nonlinear response analysis was performed by inputting the Kobe phase notification wave equivalent to level 2 earthquake to the FEM model of the embankment.

5.2.1 Analysis model

The analysis model was the same model that was used in the previous section. RO model was used for dynamic deformation characteristics of embankment and loam layer. Table 5.1 showed the reference strain and the maximum damping constant of the RO model.

Table 5.1 – Dynamic response characteristics

Reference strain $\gamma_{0.5}$	Maximum damping constant h_{max}
0.0018	0.17

5.2.2 Analysis result

Fig. 5.6 showed the distribution of maximum acceleration. Fig. 5.7 showed the Fourier spectrum ratio of the embankment (Pa1~4) to the ground (Ga1). From these results, although the amplification due to the embankment could be clearly confirmed even for strong ground motion, the tendency of the amplification at the top of slope to be particularly large was not remarkable. So, it was considered that further analysis was necessary for this tendency.

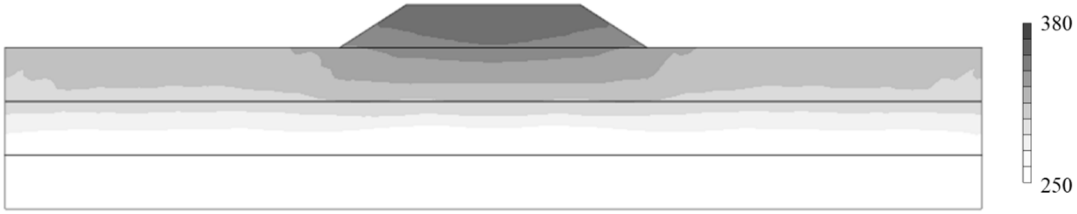

Fig. 5.6 – The distribution of maximum horizontally acceleration (*gal*)

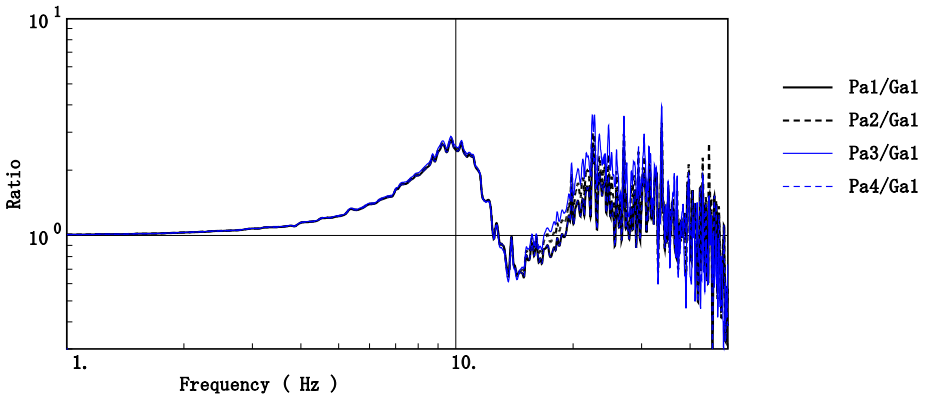

Fig. 5.7 – Fourier spectrum ratio

6. Conclusion

The main results about the characteristics of input motion for castle were follows;

(1) It is need to pay attention to underestimation due to modeling the masonry wall embankment as horizontally flat strata when the input motion of the castle was evaluated with a 1D ground model under the foundation,

(2) Regarding the seismic response of the ground, most of the castles in Japan might require attention to the above (1) when we considered the separation distance from the top of slope where the influence of embankment disappeared.

(3) The protrusion at the top of the masonry wall embankment had little effect on the earthquake response of the castle, because it had a small weight ratio to the whole embankment.

(4) There was no significant difference when we eliminated the stone weight on the surface of the masonry wall and evaluate the seismic response as a homogeneous embankment.

(5) When comparing microtremors and strong motions, the tendency of amplification at the embankment was similar. There was a difference in the tendency of amplification at the top of slope of the embankment.

Hereafter, it needs more detailed analysis since the tendency is likely to change depending on the shape of the embankment.

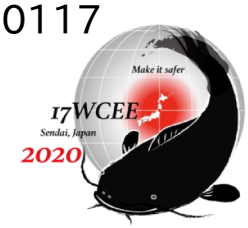

References

[1] Building Research Institute, Japan institute of country-ology and engineering (1997): Ministry of Construction Comprehensive Technology Development Project “Development of earthquake disaster prevention technology in metropolitan areas”, Earthquake motion amplification risk assessment (building) subcommittee report.

